

A COMPUTATIONAL INVESTIGATION OF MEMS - FINAL REPORT

GRANT NUMBER F49620-98-1-0027

David B. Goldstein
Center for Aeromechanics Research
Department of Aerospace Engineering and Engineering Mechanics
The University of Texas at Austin

Abstract

We applied a recently developed direct numerical simulation approach to examine MEMS for turbulent boundary layer control. We have carried out simulations of synthetic jets and textured surfaces in this first phase of the study and, in the present one-year follow-on work, are modeling concepts involving hybrid active/passive elements. We have completed a flow and geometric parameter study of synthetic jets and have produced valuable insight into the detailed physics of the actuators. In this final report we present results from simulations of periodic arrays of 2-D and 3-D pulsed synthetic jets into an initially quiescent flow, simulations of slot jets actuating beneath a turbulent boundary layer, studies on the behavior of hairpin vortices and, separately, preliminary simulations of turbulent flow over arrays of chevrons.

While the 2-D synthetic jet simulations are at much higher Reynolds numbers than needed for MEMS drag reduction in a turbulent boundary layer, they do provide a basis for comparisons with experiments and with simulations of others. The 3-D results show that the *inactive* MEMS devices have a weak effect on the boundary layer from their mere physical presence. Time averaged data show how the jet arrays affect the coherent structures of the boundary layer when activated in different combinations while instantaneous data show the formation of the three-dimensional jets in detail. In addition, we have initiated a collaborative program of study to examine the formation and evolution of hairpin vortices created with a pair of suction actuators.

Background

Recent advances have made it possible to directly simulate turbulent flow within modestly complex boundary geometries using the full Navier-Stokes equations. Such direct numerical simulation (DNS) may be used to explore the effects of fine scale surface textures and active flow controllers on a fully turbulent boundary layer. Surface modifications can have several applications but of present interest is the potential for drag reduction. Passive surface textures have been found experimentally to reduce drag by five to ten percent, as reviewed in [1] and [2]. Consequently, there is much interest in the potential of arrays of active flow manipulators for much greater drag reduction.

A turbulent boundary layer may seem to contain random fluctuations of velocity and pressure but in reality those fluctuations are associated with coherent vortical structures that arise, evolve and decay in a quasi-periodic fashion. Of particular interest are the

streamwise vortices that originate from the formation and stretching of horseshoe vortices. These vortices lead to the formation of low speed streaks which are believed to be responsible for the breakdown and eruption of the wall layer, a key mechanism in the production of new vortical structures and the increase in shear stress at the wall. Recent advances in both construction and testing have allowed experimentation with microjet MEMS (Micro Electronic Mechanical Systems) for reducing shear stress over a flat plate [3,4]. A reduction in wall shear stress has also been observed in direct numerical simulation (DNS) of turbulent channel flow subjected to an opposition control scheme [5,6] that does not include detailed actuator simulation. Although the potential of synthetic jets for flow control and viscous drag reduction had been suggested experimentally, a full DNS involving turbulent flow and the detailed physics of the jets had yet to be attempted. Simulating the internal structure of the devices is important since, as we have shown, the resulting synthetic jets are highly dependent on both the flow parameters and geometric parameters of the particular device [7].

Objectives

The objectives of the study were to use our CFD approach to investigate boundary layer control devices, to explore a range of new surface textures, and to develop a fundamental understanding of the resulting boundary layer structure. In particular we aimed to (1) model 2-D arrays of actuators for comparison to experiments at Georgia Tech, (2) model a pulse jet's impact on boundary layer coherent structures including the impact of several actuator combinations involving changes in magnitude, direction, pulsing order and frequency, and (3) examine the usefulness a few new surface textures.

Force Field Model in a Spectral Method

We use a spectral-DNS method initially developed to examine turbulent channel flow [8]. This method expands the spatial variables with Fourier and Chebyshev polynomials. Efficient transform methods are used to switch between real and spectral representations making this method attractive for its low computational cost and accuracy in simply-shaped domains. We use a localized force field to simulate stationary and moving surfaces. Such a technique allows us to utilize the fast transform methods in fairly complex geometries. This approach, detailed in [9], was used by us to successfully simulate a number of active and passive devices in fully turbulent flow [10,11]. Our results for flow over flat plates and riblets [9,10,12] have been validated against both experiments and other numerical simulations.

Modeling an Array of Two-Dimensional Actuators

Our work is distinct from other synthetic jet simulations [13,14] in both the simulation method and the problem description. In [13], a turbulence model is used to model high Reynolds number flow and the simulation concentrates mainly on the far field. In [14], the cavity is defined with a moving boundary modeling the motion of a flexible diaphragm and the internal and external flows are calculated on separate grids simultaneously. Our approach simulates a piston motion by imposing a sinusoidal-varying

streamwise velocity in a region spanning the height of the domain with the force field method. No-slip conditions are similarly used to define the slit plane. In addition, we impose a shear-free condition along the top and bottom boundaries to simulate the effect of a 2-D array of jets. We have completed parametric studies involving flow and geometric parameters and compared the results to both numerical [13,14] and experimental [15] data whenever possible. This work has appeared as an AIAA paper [7] and is about to be published in the *AIAA Journal*. The results are summarized below.

We first examined the effect of flow parameters by varying the Reynolds and Strouhal numbers. The Reynolds number is defined with the half-slit width ($Re = U_{max}(h/2)/\nu$ where U_{max} is the mean peak velocity across the slit, h is the slit width and ν the kinematic viscosity) and the Strouhal number is defined according to the piston motion ($St = \omega(h/2)/U_{max}$ where $\omega = 2\pi f$ is the angular velocity). The external flow is characterized by separation at the sharp lip and roll-up of fluid into a pair of counter-rotating vortices. The ensuing jet has no net mass flux but entrains fluid from the surrounding flow near the slit. This entrained fluid must be drawn from the right-hand side of the domain along the sides of the jet. At moderate and high Re , two distinct types of vortex pairing are observed. The first type occurs at moderate Re and consists of pairing of the first, leading vortex pair with subsequent vortices into a larger vortical structure. Once this structure propagates far downstream, the simulation reaches a steady-state in which subsequent ejected vortices dissipate before pairing can occur (figure 1). The second type of pairing occurs at high Re and consists of occasional pairing of vortices. Apparently this is a result of the complexity of the plenum flow which occasionally causes internal vorticity to be ejected through the slit, affecting the translational speed or celerity of the ejected vortices (figure 1). Variations in St substantially affect the jet formation. At low St , the piston has an effectively longer stroke with a longer actuation time. The longer stroke causes both an increase in mass ejected per cycle and impulse per unit width. Consequently, for low St , the large vortices formed remain coherent far downstream and are spaced far apart so that no pairing occurs. Conversely, at high St , the ejected vortices generated by each pulse continually merge upon exiting the cavity to form vortex sheets instead of a sequence of distinct vortices.

Inside the plenum there is a similar process of jet formation but the jet is strongly influenced by the close proximity of the piston face. The entering jet is deflected into a cavity-filling swirling motion. As noted in [14], the cavity flow becomes fairly periodic for all ranges of Re and St explored. However, unlike [14], the steady-state conditions are not reached within a few cycles, but rather after as many as 35 cycles. The complexity of the internal flow increases with Re .

We have parametrically examined the effect of lip thickness and shape and the domain dimensions. Thickening the lip around the jet aperture allows a boundary layer to develop within the aperture so that the effective slit width is reduced. As a result, the vortices form with a higher celerity and pairing, if it occurs at all, is delayed downstream.

A rounded lip produces a result intermediate between the sharp lip and a flat thick lip. A cusped lip has little effect since separation occurs at the sharp tip and is very similar to the sharp lip case. Increasing or decreasing the size of the external domain does not affect the near field appreciably: vortices do not "feel" the presence of the right-hand side wall until they are very close except due to the mean backflow feeding the entrainment.

Unlike the external flow, the internal plenum flow is not strongly affected by lip thickness or shape. However reducing the size of the cavity does cause substantial changes in the circulation cell. As the cavity becomes shallower, the primary circulation cell flattens out and allows secondary vortices to form at the edges of the cavity. For very shallow cavities, most if not all of the main circulation cell is ejected or diffused into the wall during each cycle.

Experimental results in [15] differ from ours in that an isolated real jet breaks down into smaller turbulent eddies in the vicinity of the slit. This breakdown is believed to be a consequence of 3-D instabilities not present in our 2-D simulation. In addition, spectral studies of the experimental data indicate that the jet breaks down without any pairing interactions. Aside from these differences attributable to the fact that we model 2-D periodic arrays of jets, agreement is pretty good. Our mean computational streamwise and centerline velocities, at several stations from the jet slit, match experimental data. Moreover, the vortices' trajectories also scale with the mean stroke length and period of oscillation. Also the jet centerline velocity and growth matches theoretical scaling factors near the slit. We have also modeled paired synthetic jets as in the experiments of [16] and simulations of [17]. As observed in [16], pulsing the jets in phase produces counter-rotating vortices and a jet similar to the single jet case. Preliminary studies from pulsing the jets out of phase show jet steering but the results are dominated by the narrowness of the domain in the vertical y -direction.

Micro-jet Interaction with Three-Dimensional Boundary Layer Structures

We next examined the interaction of similar micro-jets with the coherent structures in a turbulent channel flow. The goal was not so much obtaining drag reductions as understanding how realistically modeled actuators actually interact with the flow. This understanding is critical before one can hope to usefully link together huge arrays of actuators and sensors with some interaction algorithm (*e.g.*, a neural net). The domain consisted of a rectangular channel with mean flow in the x -direction. Flow was periodic in both the x and z directions while the horizontal y -planes were defined as the channel boundaries. A virtual plate 2 gridcells thick was inserted 9 gridcells above the bottom of the channel (fig. 2(a)). In the space between the plate and the lower channel wall, dividing walls spanning the length of the domain were placed to create the jet cavities such that each actuator unit consisted of two slot jets powered by a common membrane. Hence, each jet pair is coupled 180 degrees out of phase (fig. 2(b)). The dividing walls were defined as shear-free surfaces that allow parallel fluid motion but no penetration in the z -normal direction, a necessity to reduce "ghost" impressions of the internal geometry above the plate created by Gibbs phenomena. The drivers were rectangular sections of

the shear-free wall spanning the height of the cavity and measuring two slot lengths long. The devices were powered by imposing a time-varying velocity in the z-direction at the driver section of the wall. To simulate the membrane motion, the magnitude of the specified z-velocity was shaped as a sine² surface. Since the fluid was incompressible and the domain periodic in the x-direction, only spanwise sub-surface flow could create net mass fluxes in and out through such slots.

Flow Over In-active Actuators: A fully developed turbulent channel flow was used as the starting point of the simulations. The new geometry with the virtual plate and internal structure was inserted abruptly into the flow and the simulation was allowed to run for 85,000 time steps to stabilize once more with no actuation applied by the membrane. Time averaged data confirmed that the devices were essentially low profile: they did not create additional disturbances and the calculated drag was nearly identical to a flat plate.

Pulsed Jet Operation in the Absence of Channel Flow: We first tested the devices in the absence of any bulk channel motion to give insight into the characteristics of the 3-D jets. Actuation was done through a periodic sinusoidal function producing a jet with average peak velocity $7.5u^*$ at the slot plane and a corresponding device Re_{jet} of 34. This value was considerably larger than needed for boundary layer control. In later studies we used blowing speeds closer to the turbulent boundary layer turbulent fluctuations (1 to $3u^*$) but in this case the larger values were useful in visualizing jet interaction effects. Two modes of actuation were tested: the “-+-” mode with blowing jets out of the two center slots and “+--” with the jets alternating blowing and sucking. Note that as the devices continued to operate, the membranes reversed direction (due to the temporally sinusoidal membrane force field) and the opposite actuation occurred.

Results on a plane cutting through the plane of the slots are illustrated in figure 3 with the “-+-” case. The actuators produced jets with characteristics similar to 2-D arrays of synthetic jets [7]. As observed in the figure, adjacent blowing jets tend to move apart due to the proximity of the two sets of similar vortical structures and the outboard suction. The same result is seen in the 3-D jet structure shown in the isosurface of normalized vorticity (enstrophy) of figure 4. The figure also shows that, unlike other studies [14], the jet shape has thick, bulbous ends. This condition is believed to be a result of the shape of the cavity and elongated membrane: as the membrane moved, fluid near the center of the slot could readily exit the cavity. However, fluid coming from the edges of the membrane encountered an area constriction since the membrane was twice as long as the slot. Consequently, fluid was ejected more forcefully near the slot ends, leading to the end distortion in the jet shape.

Steady and Periodic Actuation: We next tested the performance of the devices in the presence of turbulent channel flow. Actuation was done through a half-step function that abruptly started and stopped the membrane motion. The membrane only actuated in one direction so the devices did not reverse direction (i.e. blowing jets only blew). Two forms of actuation were tested: “-+-” and “+--”. The jet strength was $1.5u^*$ with

a corresponding Re_{jet} of 8.2, matching the performance characteristics of experimental studies [4]. The period of oscillation (T) was 176 times larger than the viscous time scale t^* , giving a St_{jet} of 0.11 and making the actuation quasi-steady during most of the cycle. Results showed that fluid sucked into the cavity retained some streamwise momentum even below the surface while ejected fluid came out with negligible streamwise momentum. This suggests that replacing actuators with simple wall-normal boundary suction/blowing is not an adequate representation of the performance of the devices. The abrupt start of the devices generated a fair amount of vorticity but, thereafter, the jets themselves remained confined to the viscous sublayer and did not appear to substantially affect the boundary layer. However, time averaged data over 6 periods showed that different actuation modes produced distinct streak patterns. Figure 5 shows iso-surfaces of streamwise velocity corresponding to $u^+ = 4$ for both cases. The blowing “+” jets present themselves as “shark fins” deformed by convection and shearing of the mean flow. For the “-+-” case, fig. 5(a) shows the formation of two pairs of low speed streaks: a narrow and weak pair along the inside of the two outer slots and another more pronounced pair located just outside of the two outer slots. In contrast, the “+--” case (fig. 5(b)) only shows the presence of three wide low speed streaks.

To study the effect of periodic actuation in a turbulent boundary layer, we drove the “-+-” and “+--” modes with a smooth periodic actuation. The full period of oscillation (T), corresponding to a given slot going through a full cycle of blowing and sucking, was approximately $30t^*$. The continuous pulses were not independent of each other since the channel flow-through times at the centerline of the channel or even at the height of streamwise vortices ($y^+ \approx 15$) were only $85t^*$ and $154t^*$, respectively. The pumping membranes were set to generate a modestly strong jet of area-averaged peak normal velocity corresponding to $3u^*$ for a Re_{jet} of 13.6 and a St_{jet} of 0.33. These values were at the upper limit of jet strength expected to be useful for turbulent boundary layer control. Instantaneous results are illustrated in figure 6 with the “-+-” mode as iso-surfaces of normalized enstrophy in a channel section. The blowing jets are seen as the billowing structures at the center of the figure while turbulent boundary layer structures are represented by small lumps or large, elongated pancake structures. As observed previously, the center slots generated blowing jets with thick, bulbous ends which rolled up into hairpin vortices. The hairpin formation was a result of the shearing of the mean flow: as the jet rose, the leading portion reached into a higher momentum flow before the rest of the jet and rolled up into a classic hairpin vortex over the low-(streamwise) speed jet fluid. Further observation indicated that much of the low speed fluid in the body of the jet was subjected to Kelvin-Helmholtz instability which, on occasion, caused the body of the jet to roll up into a family of hairpins. Further observations on the behavior of the jets over time and for both actuation modes showed that the leading edge hairpin dominated, sometimes overtaking and swallowing weaker hairpins or leap-frogging over the trailing edge hairpin. In both cases, the leading edge hairpin interacted with the boundary layer structures and spawned several other pancake structures and occasional lifting tendrils. The jets themselves only remained coherent up to $50l^*$ above the virtual plate and $200l^*$ downstream of the location of the slots before breaking down

into other structures. While the jets dissipated quickly, their effects remained in the altered evolution of the pancake boundary layer structures as far as $1.000l^*$ downstream. Time averaged data over 80,000 time steps (80 full pumping cycles) showed that neither actuation mode created major structures in the long run. Only minor disturbances were observed throughout the channel and there were no discernible streaks. The average drags over the same long time interval were $12 \pm 5\%$ and $15 \pm 7\%$ higher than for the opposing flat wall for the “-+-” and “-+-” cases respectively. This large drag increase was not surprising in that the continuously pulsed periodic jets clearly caused strong vertical mixing of the streamwise momentum. Results for these 3-D simulations have been presented at the 2001 Reno Aerospace Sciences Meeting [18].

Single Pulses: We studied the effect of single pulses on turbulent boundary layer structures by selecting appropriate instances in which a particular structure would pass over the location of the actuators and selectively activating the devices. Two types of single actuation were tested: a steered jet and a strong jet. The steered jet was created by shaping the slots to produce a center blowing jet tilted approximately 45 degrees from the normal direction towards an adjacent suctioning slot. The strong jet consisted of a short, intense pulse of half the period and twice the magnitude of the jets used in the previous study. In both cases, a single blowing pulse was created and its interaction with the boundary layer structures was followed over several thousand time steps. Flow events and their evolution were compared to an unactuated case spanning the same time interval. In the case of the steered jet, the ejected mass of fluid rolled up into the same family of hairpin vortices previously observed. The jet was successful in disrupting the evolution of the original pancake boundary layer structure but jet itself led to the creation of a new pancake structure of similar size. Comparison of the drag for the undisturbed flow and the tiltjet over 4 periods indicate a 2% increase due to the pulse. In the case of a strong jet, the jet completely obliterated the pancake structure. However, the intense pulse also created new pancake structures and as the jet quickly rose, several rising tendril structures were left in its wake. For this case, the calculated drag over 8 periods indicated a 1.4% rise when compared to the undisturbed flow over the same period of time.

Understanding Hairpin Formation Caused by Suction Holes

In general, we have often found it difficult to cause our actuators to usefully interact with the complex 3-D turbulent coherent structures in a natural (simulated) boundary layer. The jets or sink regions we produce tend to introduce new vorticity or at least cause greater vertical mixing of the flow with a consequent drag increase. In order to better understand the nature of the vorticity introduced by such actuators, we have begun to model the interaction of a pair of simple suction holes with a laminar flow. This work has led to a new collaboration with Prof. Jacob Cohen at the Technion in Israel who has been exploring such flows experimentally. With the additional support of a Lady Davis Fellowship from the Technion and a Dean's Fellowship from UT, I traveled to Haifa in Fall, 2000, to begin simulations with our code to model such flows.

Under certain circumstances an adjacent pair of suction holes below a simple flat-plate laminar boundary layer produces a train of hairpin vortices through a highly non-linear process (fig. 7). Such hairpins are likely essential building blocks of more general coherent structures in a turbulent boundary layer. When we use an array of actuators for drag reduction, we certainly do not want to introduce trains of hairpins or similar structures which will grow into concentrated turbulent knots. Hence, we have been considering the flow induced by the most simple possible array of actuators, a pair of suction holes producing steady suction, to study the effects of geometric and flow parameters on the nature of the resultant wake.

Modeling New Surface Textures

Results in [19] indicate that surface textures resembling randomly aligned rows of chevrons of height $O(7l^*)$ could produce dramatic drag reduction in turbulent channel flow. We have now completed several DNS runs of similar configurations. We have explored different random and regular orientations and a couple of different chevron shapes but so far we have been unable to obtain reductions in drag. We have sponsored a simplified version of the work in as an undergraduate project to measure drag on a chevron-coated-flat-plate with a pitot rake [20]. However, preliminary results have also not found any substantial drag reduction. We are continuing to work on these simulations and expect to present results in the near future.

References

- [1] M. J. Walsh, 1990, "Riblets." In *Viscous Drag Reduction in Boundary Layers*, ed. D. Bushnell and J. Hefner, Progress in Astronautics and Aeronautics, v. 123, p. 203-259, AIAA Washington, DC.
- [2] E. Coustols and A. M. Savill, 1992, "Turbulent skin-friction drag reduction by active and passive means: parts 1 and 2," Special course on skin-friction drag reduction, p. 8-1 to 8-55, March 2-6, in AGARD Report 768.
- [3] C. M. Ho, S. Tung, G. B. Lee, Y-C Tai, F. Juang, and T. Tsao, 1997, "MEMS - A technology for advancements in aerospace engineering," AIAA paper 97-0545, *35th Aerospace Sci. Meet.*, Reno, NV, January 1997.
- [4] K. S. Breuer and K. Amonlirdviman, 1999, "Advances in Feed-Forward Control of Turbulent Boundary Layers," AIAA Paper 99-3401, *30th AIAA FLuid Dyn. Conf.*, Norfolk, VA, June 1999.
- [5] H. Choi, P. Moin and J. Kim, 1994, "Active Turbulence Control for Drag Reduction in Wall-Bounded Flows," *J. Fluid Mech.*, **262**, 75.
- [6] P. Koumoutsakos, T. Bewley, E. P. Hammond and P. Moin, 1997, "Feedback Algorithms for Turbulence Control - Some Recent Developments," AIAA paper 97-2008, *35th Aerospace Sci. Meet.*, Reno, NV, January 1997.
- [7] C. Lee and D. B. Goldstein, 2000, "Two-Dimensional Synthetic Jet Simulation," AIAA paper 2000-0406, *38th Aerospace Sci. Meet.*, Reno, NV, January 2000.

- [8] J. Kim, P. Moin, and R. Moser, 1987. "Turbulence statistics in fully developed channel flow at low Reynolds number." *J. Fluid Mech.*, **177**, 133.
- [9] D. B. Goldstein, R. Handler, and L. Sirovich, 1995. "Direct numerical simulation of turbulent flow over a modeled riblet covered surface." *J. Fluid Mech.*, **302**, Nov. 10, 333-376.
- [10] D. B. Goldstein and T.-C. Tuan, 1998. "Secondary flow induced by riblets." *J. Fluid Mech.*, **363**, pp. 115-151.
- [11] T.-C. Tuan and D. B. Goldstein, 1996, "Direct numerical simulation of arrays of microjets to manipulate near wall turbulence," U. T. Austin Center for Aeromechanics Research Report CAR-96-3
- [12] D. B. Goldstein, R. Handler, and L. Sirovich, 1993, "Modeling a no-slip flow boundary with an external force field," *J. Comp. Phys.*, **105**, pp. 354-366.
- [13] L. Kral, J. Donovan, A. Cain and A. Cary, 1997, "Numerical simulations of synthetic jet actuators," AIAA Paper 97-1824 *28th AIAA Fluid Dyn. Conf.*, Snowmass CO, AIAA paper 97-1824.
- [14] D. P. Rizzetta, M. R. Visbal, and M. J. Stanek, 1998, "Numerical investigation of synthetic jet flowfields," AIAA paper 98-2910, *29th Fluid Dyn. Conf.* Albuquerque, NM, June 1998.
- [15] B. L. Smith and A. Glezer, 1998. "The Formation and Evolution of Synthetic Jets," *Physics of Fluids*, Vol. **10**, No. **9**, pp. 2281-2297.
- [16] B. L. Smith, M. A. Trautman and A. Glezer, 1999. "Controlled Interactions of Adjascent Synthetic Jets," AIAA Paper No. 99-0669, *37th AIAA Aerospace Sciences Meeting*, Reno, NV, January 1999.
- [17] L. Kral, D. Guo, 1999, "Characterization of Jet Actuators for Active Flow Control," AIAA Paper 99-3573, *30th AIAA Fluid Dyn. Conf.*, Norfolk, VA, June 1999.
- [18] C. Lee and D. B. Goldstein, 2001. "DNS of Microjets for Turbulent Boundary Layer Control," AIAA paper 2001-1013, *39th Aerospace Sci. Meet.*, Reno, NV, January 2001.
- [19] L. Sirovich and S. Karlsson, 1997, "Turbulent Drag Reduction by Passive Mechanisms," *Nature*, Vol. **388**, pp. 753-755.
- [20] A. Braun and T. Fitzgerald. "The Effects of Passive Mechanisms on the Turbulent Drag of a Flat Plate," Presented at the 1999 AIAA Southwest Regional Student Paper Competition, Albuquerque, NM, April 1999.

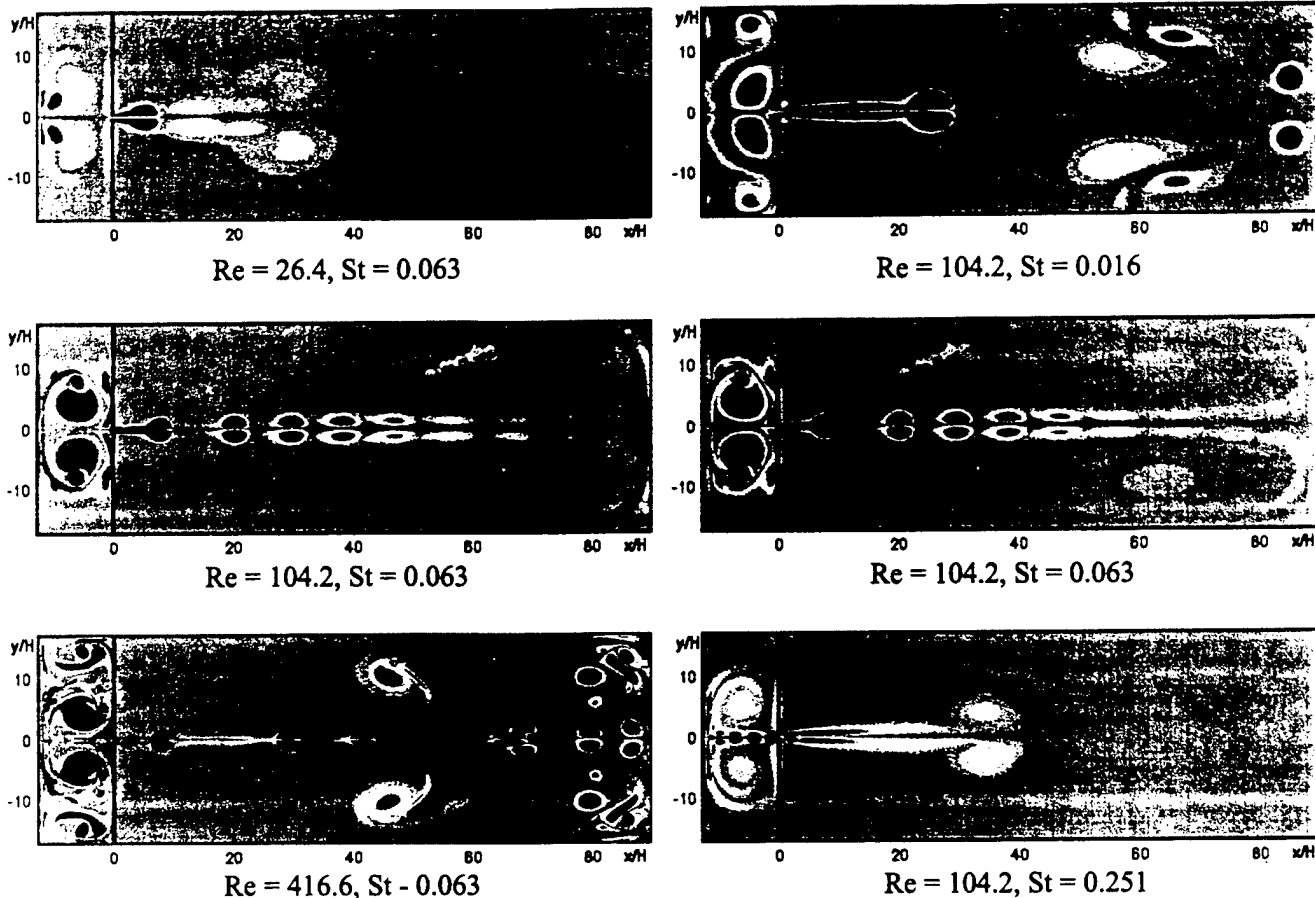
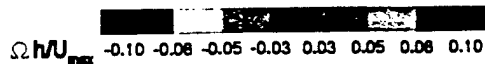


Figure 1: Vorticity Contours of 2-D arrays of synthetic jets for varying flow parameters

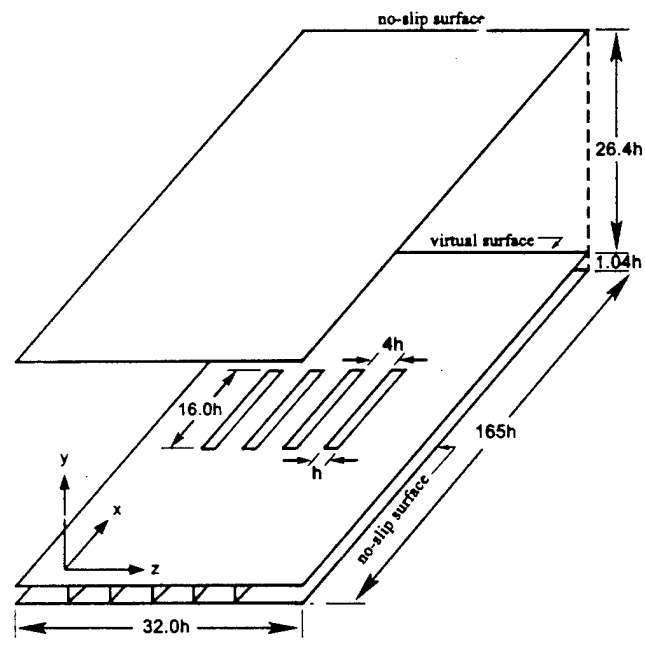


Figure 2(a): Schematic of channel and actuators

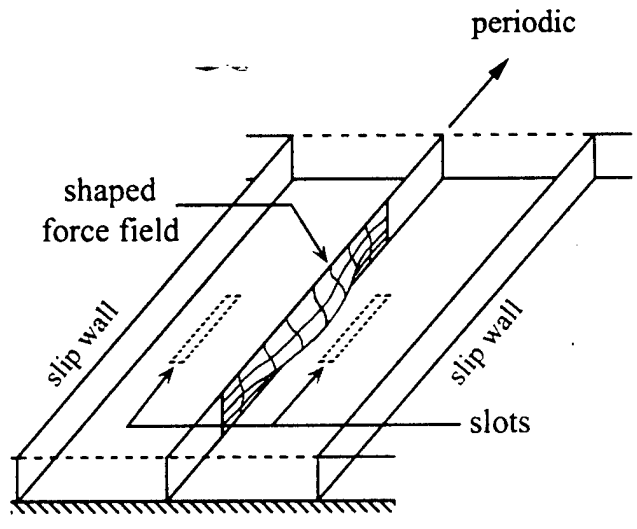


Figure 2(b): Schematic of single actuator array and sample force field shape for membrane deformation

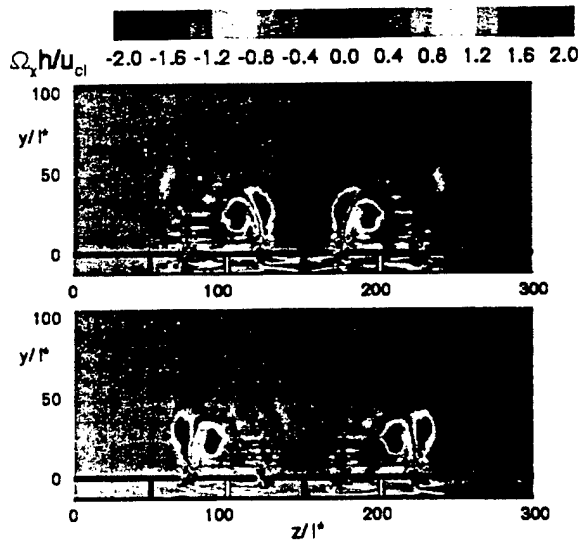


Figure 3: Contours of normalized Ω_x vorticity on zy -plane through actuators for no mean channel flow (top = "-+-" actuation, bottom = "+-+" actuation)

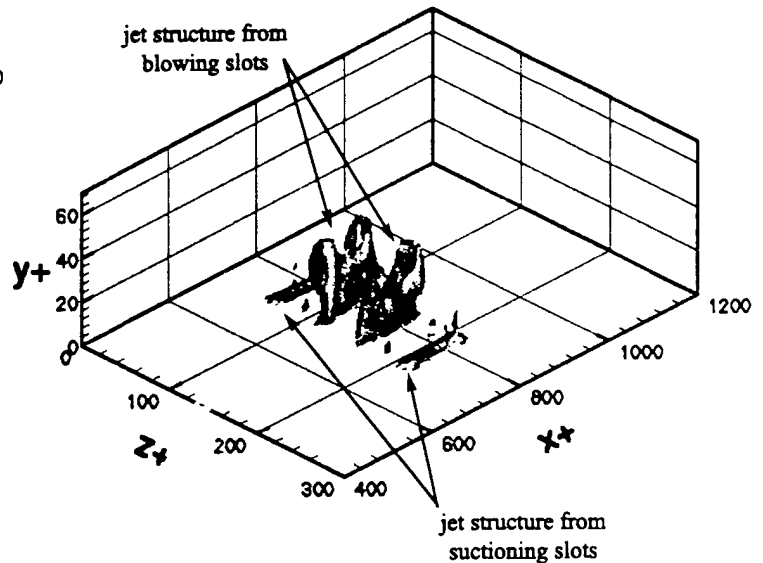


Figure 4: Contours of normalized instantaneous enstrophy for "-+-" actuation at $T/2$ ($|\underline{\Omega}| h/u_{cl} = 2$)

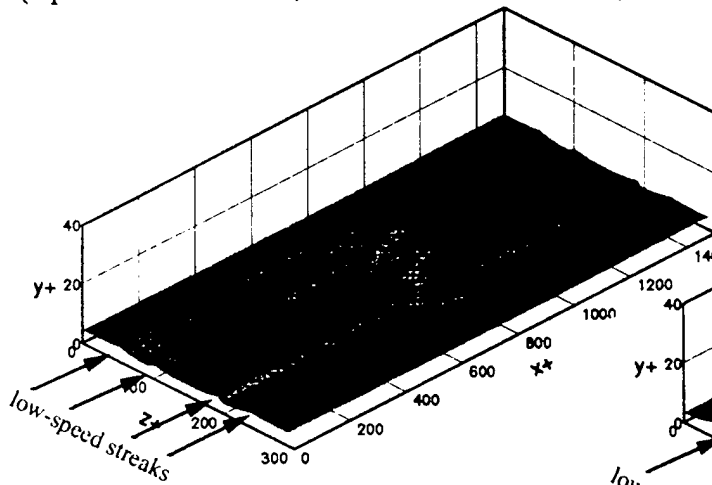


Figure 5(a): Time averaged iso-surface of streamwise vel. ($u^+ = 4$) for quasi-steady "-+-" actuation

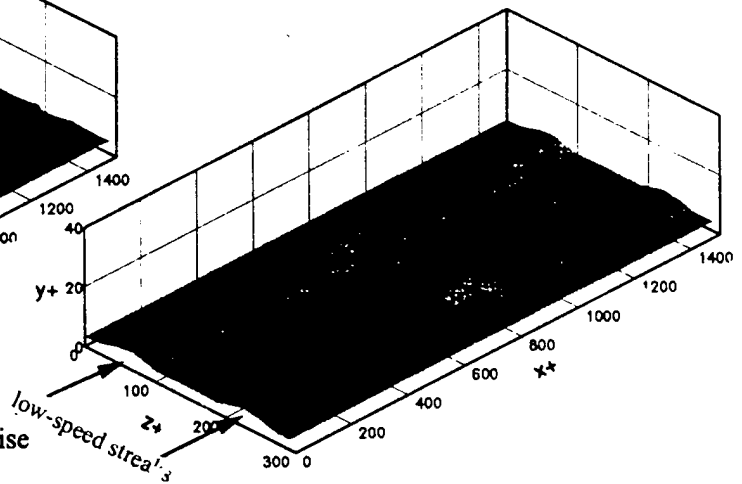


Figure 5(b): Time averaged iso-surface of streamwise vel. ($u^+ = 4$) for quasi-steady "+-+" actuation

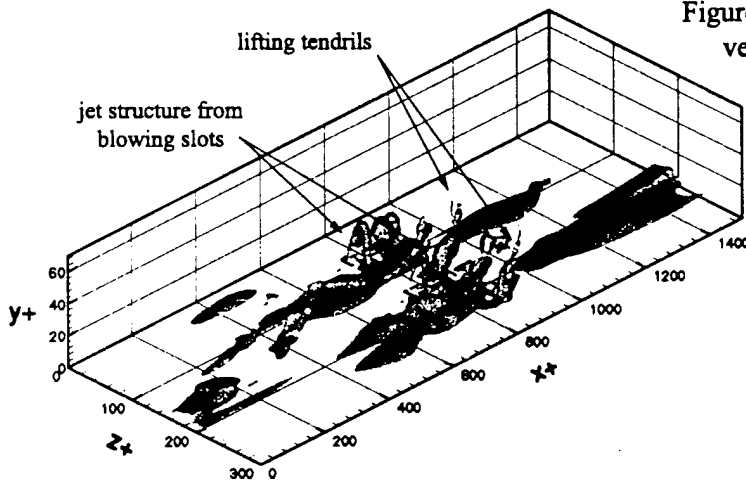


Figure 6: Contours of normalized instantaneous enstrophy for continuously pulsed "-+-" mode at $t = 3T$ ($|\underline{\Omega}| h/u_{cl} = 2$)

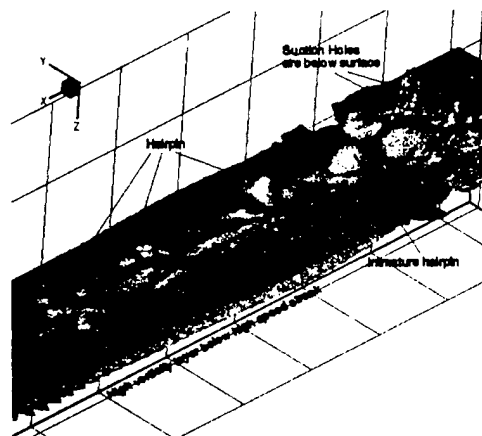


Figure 7: Iso-surfaces of Ω_x showing hairpins shedding in the wake of two holes (flow from upper right)